The effect of post-annealing on the structure and magnetotransport properties of $Pr_{0.5}Sr_{0.5}MnO_3$ thin film

Liping Chen,[1,2,a] Jiali Zeng,[2] Miao Li,[1] Zhenhua Tang,[2] and Ju Gao[2,a]
[1]*Department of Physics, Zhejiang Normal University, Jinhua 321004, People's Republic of China*
[2]*Department of Physics, Chong Yuet Ming Physics Building, The University of Hong Kong, Pokfulam Road, Hong Kong, Hong Kong*

(Presented 1 November 2016; received 22 September 2016; accepted 28 November 2016; published online 13 March 2017)

$Pr_{0.5}Sr_{0.5}MnO_3$ (PSMO) thin film is epitaxially grown on (001)-oriented $LaAlO_3$ single-crystal substrate using pulsed laser deposition (PLD). It is found that the as-grown PSMO film shows compressive strain in plane and tensile strain out of the plane. Upon annealing at 900°C in the air, the strain is significantly relaxed. The paramagnetic to ferromagnetic phase transition temperature T_C shifts from 200 K to 220 K, and the antiferromagnetic insulating phase is suppressed in the phase separated state at low temperature. In addition, the magnetoresistance (MR) is found to increase around the ferromagnetic transition temperature, whereas it decreases from 99% to 60% at low temperature of 20 K. [http://dx.doi.org/10.1063/1.4978634]

I. INTRODUCTION

The manganite $R_{1-x}A_xMnO_3$ (R = rare earth ion; A = divalent alkaline earth metal ion) has shown lots of remarkable phenomena such as magnetoresistance (MR), Jahn-Teller effect, and phase separation.[1–4] The half-doped manganite $Pr_{0.5}Sr_{0.5}MnO_3$ (PSMO) is an attractive material exhibiting a multicritical phase diagram, which includes paramagnetic insulating (PMI), ferromagnetic metallic (FMM), antiferromagnetic insulating (AFI) as well as charge ordered (CO) states, and has a natural tendency towards phase separation/competition.[4–8] Therefore, the transport properties of the PSMO are sensitive to external stimuli like magnetic field, substrate-induced strain and grain size.[8–15] Both the growth orientation and strain affect the phase diagram of the film. The films on (110)-oriented substrates like $SrTiO_3$ (STO) and $LaAlO_3$ (LAO) have two phase transitions upon cooling, from PMI to FMM and then to AFI state.[8–13] In contrast, the (001)-oriented film is absent of AFI phase. Tensile or compressive strain is another factor that could enhance the AFI phase. The FMM-AFI phase transition is observed in the greatly strained (001)-oriented films and the transition temperature decreases with increasing thickness due to strain relaxation.[14–16] In order to obtain strained epitaxial (001)-oriented PSMO film on LAO substrate, the growth temperature should be higher than 700°C. Otherwise the film shows no significant strain and does not exhibit the AFI phase.[16]

Post-annealing is usually used to improve crystallization of the films, and it could strongly affect the electrical and magnetic properties. However, the effect of post-annealing ons the properties of PSMO film has not been thoroughly studied. In this paper, the effect of annealing on the PSMO film grown on the (001)-oriented LAO single-crystal substrate is thoroughly investigated. The paramagnetic to ferromagnetic phase transition temperature T_C shifts from 200 K to 220 K, and the antiferromagnetic insulating phase is suppressed at low temperature.

[a]E-mail: chenliping0003@163.com, jugao@hku.hk

II. EXPERIMENTAL

PSMO thin film was grown on (001)-oriented LAO single-crystal substrate by PLD. During the deposition, the substrate was kept at a temperature of 700°C, and the oxygen pressure was kept at 30 Pa. In order to reduce oxygen vacancy, the film remained in oxygen of 0.5 atm at the deposition temperature for 5 minutes before cooling down to room temperature.

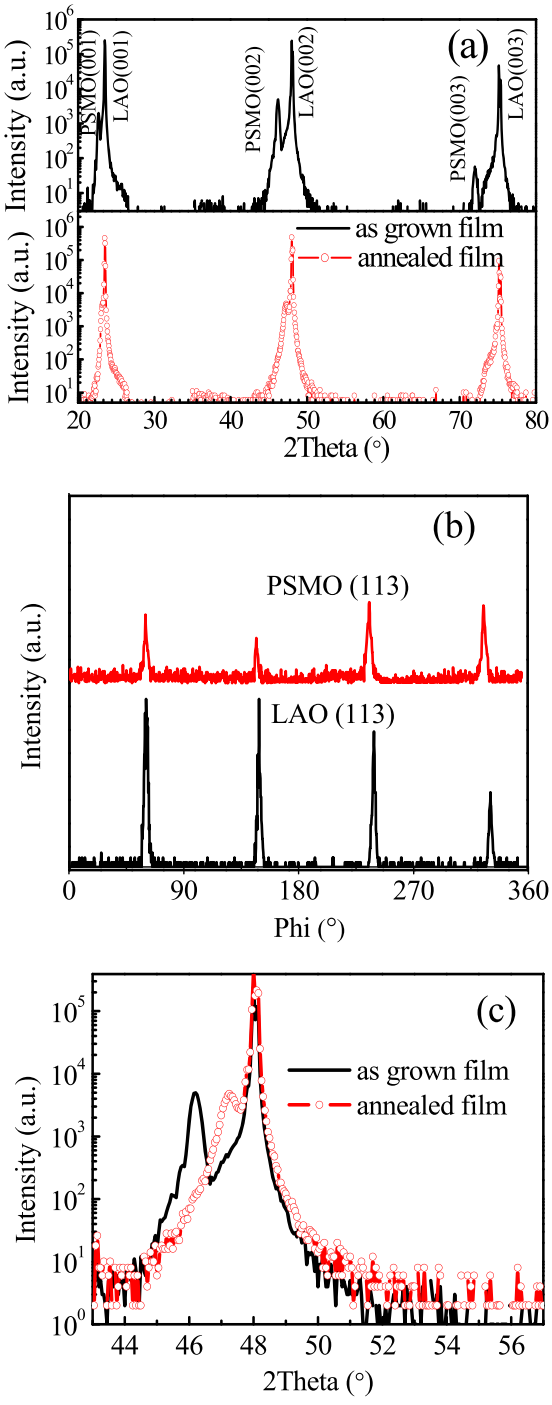

FIG. 1. XRD patterns of PSMO thin film: θ-2θ pattern of the as-grown film (a); φ scan patterns of LAO substrate (113) and PSMO film (113) along the 001 direction for the as-grown film (b); θ-2θ scan curves of (002) PSMO plane for the as-grown film (line) and annealed film (circle) (c).

The as-grown film was then annealed at 900°C in air for 2 hours after structural and transport measurements.

The crystal structure of the film before and after the annealing was detected by x-ray diffraction (XRD). The temperature dependent resistivity (ρ-T) was measured by physical property measurement system (PPMS) using a standard four-probe method. The magnetization versus temperature (M-T) was measured by superconducting quantum interference device (SQUID) with zero-field-cooled (ZFC) field warming and field-cooled (FC) runs applying a magnetic field of 5 T parallel to the substrate plane. The film thickness, as controlled by deposition time, was measured by a Dektak stylus profiler. The films studied in this paper have a thickness of ~ 30 nm.

III. RESULTS AND DISCUSSION

Figure 1(a) shows the XRD spectra of the as-grown PSMO film (line) and annealed film (circle). Only peaks from (00l) reflection of LAO substrate and PSMO film are observed in the normal θ-2θ scans and no other peaks can be observed, demonstrating that the PSMO film is highly epitaxial and of single phase. The formed ABO_3 phase has the c-axis perpendicular to the substrate surface. The 0-360° φ scan patterns of LAO substrate (113) and PSMO film (113) along the 001 direction are presented in Figure 1(b). A tetragonal structure with an epitaxial relationship of PSMO 100 //LAO 100 can be examined. Upon annealing at 900°C, the offset of the PSMO (002) peak shifts towards a larger angle, i.e., from 46.15° to 47.25°, as shown in the Figure 1(c). This indicates a decrease of the out-of-plane lattice c from 0.393 nm to 0.384 nm. The mismatch between the LAO

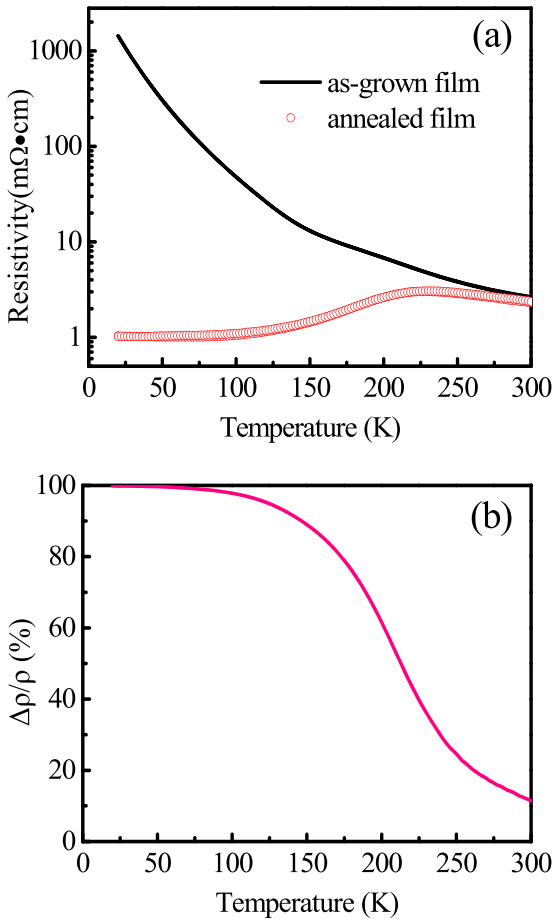

FIG. 2. The temperature dependent resistivity of the as-grown film (line) and annealed film (circle) (a) and the resistivity change of $\Delta\rho/\rho(\%)=(\rho_{\text{as-grown film}}-\rho_{\text{annealed film}})/\rho_{\text{as-grown film}}\times100\%$ (b).

substrate (cubic, ~0.379 nm) and PSMO (pseudocubic, ~0.384 nm[17,18]) suggests the epitaxial film is subjected to a compressive strain in plane. Considering the Poisson's ratio an elongation along the direction perpendicular to the surface will be induced. The out-of-plane lattice of as-grown film is much larger than that of the bulk material, indicating that the film is greatly strained. The lattice constant of the annealed film is greatly decreased, and very close to its bulk value. The full-width at half-maximum (FWHM) of the PSMO (002) peak of the as-grown film and the annealed film are almost the same (~0.35°). This suggests that the crystalline domains are small in size and does not change significantly upon annealing (~23 nm[19]).

Figure 2(a) shows the temperature dependence of resistivity for the as-grown film (line) and the annealed film (circle). The as-grown film exhibits an insulator characteristic, i.e., its resistivity increases with decreasing temperature; whereas the annealed film shows an insulator-metal transition with a resistivity peak at 230 K, and is metallic at lower temperature. To describe the resistivity changes induced by annealing, we define the resistivity ratio between the as-grown film and annealed film. As shown in Figure 2(b), the $\Delta\rho/\rho(\%)=(\rho_{\text{as-grown film}}-\rho_{\text{annealed film}})/\rho_{\text{as-grown film}}\times 100\%$ increases with decreasing temperature (from 11.4% at room temperature to 99.9% at 20 K).

Figure 3(a) is the temperature dependence of the magnetization M-T of the as-grown film (line) and annealed film (circle). As magnified in the inset of Figure 3(a), the as-grown film has a paramagnetic-ferromagnetic transition at around 200 K and a ferromagnetic-antiferromagnetic transition at around 110 K, as the magnetization in both FC and ZFC M-T curves begins to decrease at this temperature. The magnetization at low temperature is far above zero, implying the coexistence

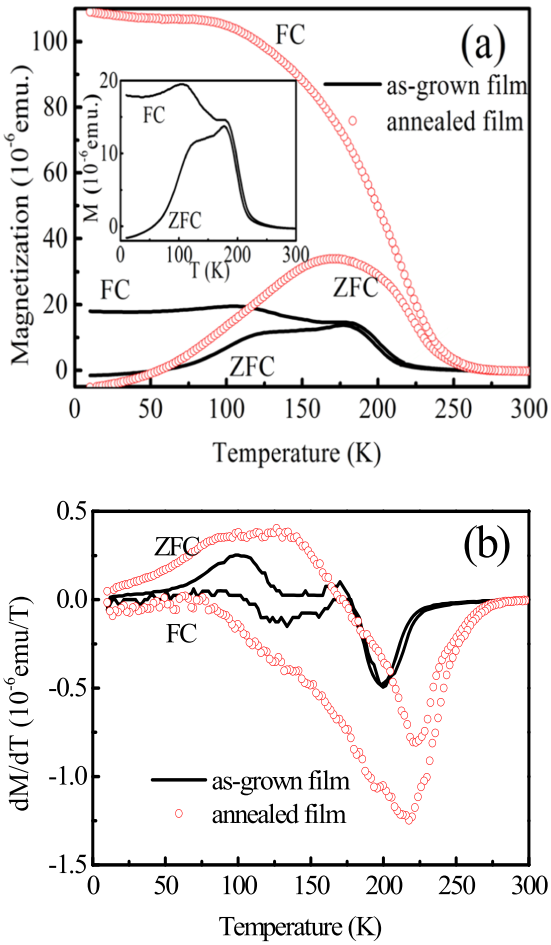

FIG. 3. M-T curves (a) and the dM/dT-T (b) of as-grown film (line) and annealed film (circle). The M-T curve of the as-grown film were magnified in the inset of Figure 3(a). The arrows mark the changes of transition temperature.

of the FMM phase and AFI phase. For the annealed film, the magnetization increases quickly at 220 K, indicating a paramagnetic-ferromagnetic transition at this temperature. Though the magnetization turns slowly raises below the temperature of 100 K, the magnetization is still unsaturated till 20 K. Comparing to the as-grown film, the annealed film has a wider FM phase-transition temperature range. In addition, the magnetization is greatly enhanced in magnitude especially at low temperature. Figure 3(b) shows the relationship between dM/dT and T. The Curie temperature increases from 200 K for the as-grown film to 220 K for the annealed film.

Figure 4 is the resistivity change versus magnetic field (a) and the related MR=[ρ(0) -ρ($\mu_0 H$=5T)]/ρ(0)*100% (b) of the as-grown film (square) and the annealed film (circle). The MR of the as-grown film rises quickly with decreasing temperature below the ferromagnetic transition. At low temperature near 20 K the MR reaches 99.2% under a magnetic field of 5 T. The annealed film undergoes a metal-to-insulator transition around 230 K without magnetic field. With a magnetic field of 5 T, the metal-to-insulator transition temperature increases to 280 K, similar to what is found in many manganite film involving ferromagnetic transitions. Comparing with the as-grown film, the annealed film shows various MR dependent on temperature. The MR is enhanced above the FM transition temperature ~220 K but greatly suppressed below the temperature. The MR of annealed film is only 59.7% at 20 K, much lower than that (99.2%) of the as-grown film.

After post-annealing, the out-of-plane lattice constant goes down to a bulk value. It seems that the interface strain has been totally released by annealing. However, during the annealing the oxygen vacancies may be modified, which would also modulate the lattice parameter, and consequently the

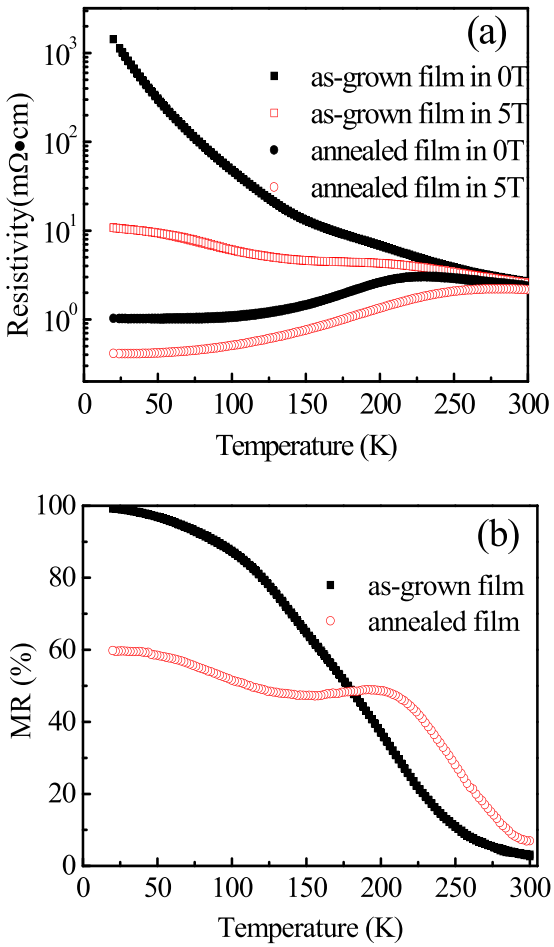

FIG. 4. The resistivity under various magnetic field (a) and MR=[ρ(0)-ρ($\mu_0 H$=5T)]/ρ(0)×100% (b) of the as-grown film (square) and annealed film (circle).

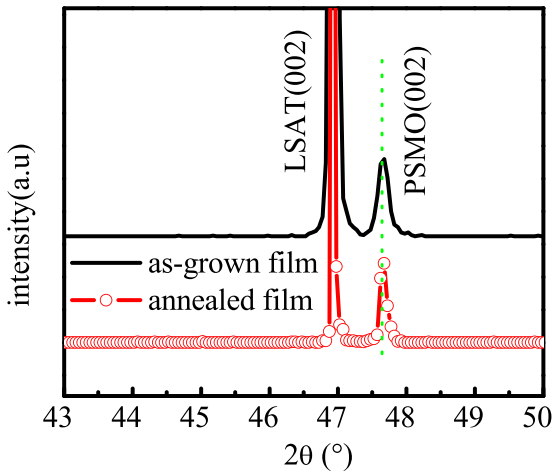

FIG. 5. XRD patterns of PSMO film on (001) LSAT before and after annealing.

electric/magnetic properties of manganite film.[21,22] For example, the filling of oxygen vacancies may lead to a decrease of volume of lattice, the drop of resistivity and enhancement of insulator-metal transition temperature.[23,24] To distinguish strain effect from the change of oxygen deficiency induced by the annealing, we studied the influence of annealing on PSMO thin film deposited on (001)-oriented $(LaAlO_3)_{0.3}$–$(SrAl_{0.5}Ta_{0.5}O_3)_{0.7}$(LSAT) substrates with identical conditions.

As the lattice of LSAT and PSMO is very close, the film on LSAT is little strained.[14] In this film, strain relaxation may rarely take place in the annealing. As a result, the possible changes of the oxygen vacancies could be detected by comparing the properties of this film before and after annealing. Figure 5 shows the XRD of PSMO thin film on (001)-oriented LSAT substrate before and after annealing. The reflection peak of (002) PSMO is at the same angle, indicating the out-of-plane lattice is little modified in the annealing. This observation shows that the oxygen vacancy changes in the annealing is not obvious. As previously described, to reduce oxygen vacancy the films are remained in oxygen of 0.5 atm at the deposition temperature for 5 minutes. Considering this treatment the little change of oxygen vacancy in annealing is comprehensible.

Two types of MR phenomena in various manganite materials have been revealed: (i) at the Curie temperature region, a somewhat 'standard' MR1 effect takes place since small field can easily align the moments of the ferromagnetic islands of random orientation, leading to a percolative conductor; (ii) at low temperatures where the system is insulating, a huge MR is detected as well. Such MR2 originates from the competition between FMM phase and AFI phase.[20] These two types of MR phenomena are both found in the as-grown PSMO film (from PMI to FMM, and then to AFI) upon cooling. The annealing induced great changes of magnetotransport. This might be ascribed to the strain effect on the phase separation among PMI, FMM and AFI. With strain relaxation, the ferromagnetic phase is enhanced. The shift of the PMI-AFI transition to higher temperature, together with the enhancement of magnetization and conductivity, demonstrated that post-annealing has led to the increase of the proportion of FM phase. With more ferromagnetic island, the percolative conductive channel could be realized with smaller magnetic field, resulting in MR1. On the contrary, the strain relaxation weakens the AFI phase. Considering the MR2 is mostly caused by the AFI-FMM transition, the large decrease of the MR at low temperature is understandable, as there is less area of AFI phase contributing to the AFI-FMM transition.

IV. CONCLUSIONS

Epitaxial PSMO thin film is grown on (001)-oriented LAO single-crystal substrate by PLD. The effect of post-annealing on the lattice structure and electrical properties are thoroughly investigated and discussed. The annealed film shows decreased resistivity and enhanced magnetization. Two types of MR are discussed and it is suggested to be due to the strain effect on phase separation.

ACKNOWLEDGMENTS

The work has been supported by the National Science Foundation of China (No. 11304285), the National Key Project for Basic Research of China (No. 2014CB921002) and the Research Grant Council of Hong Kong (Project Code No. 702112).

[1] M. Tokunaga, Y. Tokunaga, and T. Tamegai, Phys. Rev. Lett. **93**, 037203 (2004).
[2] A. J. Millis, P. B. Littlewood, and B. I. Shraiman, Phys. Rev. Lett. **74**, 5144 (1995).
[3] Y. Tomioka, A. Asamitsu, Y. Moritomo, H. Kuwahara, and Y. Tokura, Phys. Rev. Lett. **74**, 5108 (1995).
[4] K. J. Lai *et al.*, Science **329**, 190 (2010).
[5] S. Mori, C. H. Chen, and S. W. Cheong, Nature **392**, 473 (1998).
[6] L. P. Chen, X. X. Guo, and J. Gao, J Magn. Magn. Mater. **405**, 249 (2016).
[7] A. Mukherjee, W. S. Cole, P. Woodward, M. Randeria, and N. Trivedi, Phys. Rev. Lett. **110**, 157201 (2013).
[8] Y. Uozu *et al.*, Phys. Rev. Lett. **97**, 037202 (2006).
[9] J. F. Wang, L. P. Chen, Y. C. Jiang, and J. Gao, J. Appl. Phys. **113**, 17E151 (2013).
[10] L. Hu *et al.*, J. Appl. Phys. **106**, 083903 (2009).
[11] Y. Ogimoto *et al.*, Appl. Phys. Lett. **86**, 112513 (2005).
[12] Y. Wakabayashi *et al.*, J. Phys. Soc. Jap. **77**, 014712 (2008).
[13] A. Biswas, I. Das, and C. Majumdar, J. Appl. Phys. **98**, 124310 (2005).
[14] L. P. Chen *et al.*, J. Magn. Magn. Mater. **324**, 1189 (2012).
[15] L. P. Chen, F. Wang, Y. S. Chen, Y. Sun, and J. Gao, Euro. Phys. Lett. **100**, 47006 (2012).
[16] W. Prellier and B. Mercey, J. Phys. D **38**, 172, (2005).
[17] A. Llobet, J. L. Garcia-Munoz, C. Frontera, and C. Ritter, Phys. Rev. B **60**, R9889 (1999).
[18] R. Kajimoto, H. Yoshizawa, Y. Tomioka, and Y. Tokura, Phys. Rev. B **66**, 180402(R) (2002).
[19] B. E. Warren, Diffraction of imperfect crystallites in *X-Rays Diffraction* (New York: Dover) 251 (1969).
[20] H. Aliaga, D. Magnoux, A. Moreo, D. Poilblanc, S. Yunoki, and E. Dagotto, Phys. Rev. B **68**, 104405 (2003).
[21] Y. S. Du, B. Wang, T. Li, D. B. Yu, and H. Yan, J. Magn. Magn. Mater. **297**, 88 (2006).
[22] R. Patterson, C. Ozeroff, K. H. Chow, and J. Jung, Appl. Phys. Lett. **88**, 172509 (2006).
[23] J. R. Sun, C. F. Yeung, K. Zhao, L. Z. Zhou, C. H. Leung, H. K. Wong, and B. G. Shen, Appl. Phys. Lett. **76**, 1164 (2000).
[24] T. R. Gopalarao, S. Ravin, and D. Pamu, J. Magn. Magn. Mater. **409**, 148–154 (2016).